NACA RM E54H17

NACA

RESEARCH MEMORANDUM

INVESTIGATION OF A HIGH-PRESSURE-RATIO EIGHT-STAGE AXIAL-FLOW RESEARCH COMPRESSOR WITH TWO TRANSONIC INLET STAGES

III - INDIVIDUAL STAGE PERFORMANCE CHARACTERISTICS

By Charles H. Voit and Richard P. Geye

Lewis Flight Propulsion Laboratory
Cleveland, Ohio

NATIONAL ADVISORY COMMITTEE
FOR AERONAUTICS

WASHINGTON

November 1, 1954
Declassified September 17, 1958

NATIONAL ADVISORY COMMITTEE FOR AERONAUTICS

RESEARCH MEMORANDUM

INVESTIGATION OF A HIGH-PRESSURE-RATIO EIGHT-STAGE AXIAL-FLOW RESEARCH COMPRESSOR WITH TWO TRANSONIC INLET STAGES

III - INDIVIDUAL STAGE PERFORMANCE CHARACTERISTICS

By Charles H. Voit and Richard P. Geye

3393

CI-1

SUMMARY

The individual stage performance was determined for an eight-stage axial-flow compressor from circumferentially fixed radial rake measurements of total temperature and total pressure at the discharge of each stage. The performance of stages 1, 3, 4, 5, and 6 was as anticipated in design and produced a peak pressure ratio considerably above the design pressure ratio. Stages 2, 7, and 8 produced a peak pressure ratio approximately equal to design. The stages of this compressor were mismatched at design speed because of an excessive design boundary-layer allowance in the latter stages, which caused stages 7 and 8 to stall before the design over-all pressure ratio could be obtained. Between 80 and 90 percent of design speed, the stages were well matched and a peak efficiency of approximately 0.87 resulted. The excessive design boundary-layer allowance in the latter stages affected the low-speed performance favorably, and a relatively high part-speed efficiency was obtained. The knee in the surge line at 63 percent of design speed corresponded to the point at which the first stage came out of stall. It appears that the stall of the first stage at low speeds adversely affected the performance of stages 2 to 5.

INTRODUCTION

In the design of axial-flow compressors with high over-all pressure ratios, the matching of the stages may seriously affect the design and off-design performance. In the design of the compressor of references 1 and 2, as in most axial-flow compressor designs, an attempt was made to match all the stages at or near their minimum-loss points at the over-all compressor design point.

The over-all performance of this compressor (refs. 1 and 2) showed that at design speed the peak total-pressure ratio and efficiency were

somewhat below the design values. Reference 2 indicated that, based on the meager data available, the low pressure ratio and efficiency were due to mismatching of the stages at design speed, probably because of an excessive design boundary-layer allowance in the latter stages of the compressor. It was also indicated that at part speed the decrease in compressor efficiency and the knee in the surge line were less than might be expected from an analysis such as that presented in reference 3. The stages were better matched at some speed below design, which would improve the low-speed performance.

3393

In order to determine more definitely the causes of the over-all performance characteristics and to extend the over-all study of the eight-stage compressor of references 1 and 2, this investigation was conducted at the NACA Lewis laboratory to determine the performance of the individual stages. From the individual stage performance characteristics, the matching of these stages and the effect of both stage matching and stage performance on the over-all compressor characteristics were evaluated. Radial rake measurements of total pressure and total temperature were obtained after each stage for flows ranging from choke to the approximate compressor stall limit over a range of speeds from 30 to 100 percent of equivalent design speed.

SYMBOLS

The following symbols are used in this report:

A	annulus area, sq ft
P	total pressure, in. Hg abs
Q	volume flow, cu ft/sec
T	total temperature, $^{\circ}R$
U	wheel speed, ft/sec
V	velocity relative to first rotor
W	weight flow, lb/sec
δ	ratio of total pressure to standard NACA sea-level pressure
η	adiabatic temperature-rise efficiency
θ	ratio of total temperature to standard NACA sea-level temperature

μ viscosity, lb/(ft)(sec)

ρ static density, lb/cu ft

Subscripts:

e equivalent, indicates that the parameter to which it is affixed has been corrected to design speed

m mean annular radius

n station number

0 inlet depression-tank station

3,5,....17 interstage instrument stations at exit of first, second,.... eighth stators

20 discharge measuring station

3393

CJ-1 back

APPARATUS AND INSTRUMENTATION

The 20-inch-tip-diameter eight-stage axial-flow compressor reported in references 1 and 2 and schematically shown in figure 1 was used for the investigation. The test installation and instrumentation for the determination of over-all performance are the same as those presented in reference 2. In addition, interstage instrumentation was installed at the axial locations shown in figure 1. A single radial total-pressure rake (fig. 2(a)) and a single radial total-temperature rake calibrated for Mach number (fig. 2(b)) were used after each stator blade row. In order to minimize flow-angularity effects, the rakes were located behind stator blade rows and between blade wakes, where changes of flow angles are relatively small over a wide range of flow conditions. As a further precaution, shielded total-pressure probes, which are insensitive to angles of yaw up to $\pm 40^{\circ}$, and spike-type thermocouples, which are insensitive to yaw angles of $\pm 10^{\circ}$, were used on the rakes. The rakes in the first five stages had five measuring tips each, and the rakes in the last three stages had three tips each, located at area centers of equal annular areas. Instruments were placed around the periphery of the compressor so that they would not be in the wakes of the preceding instruments. The pressure measurements were photographed from mercury manometers, and the difference between the temperature at each stage outlet and the temperature in the depression tank was measured on a self-balancing potentiometer.

PROCEDURE

The compressor was operated at speeds from 30 to 100 percent of equivalent design speed. At each speed a range of air flow was investigated

from the maximum flow at which the compressor was choked to a minimum flow approximately at the point of incipient surge. The inlet pressure was varied to maintain an approximately constant Reynolds number of 1,000,000 relative to the first rotor at all speeds except 30 and 50 percent of design. The Reynolds number is defined as $\rho V l/\mu$, where the characteristic length l is the chord of the first rotor blade at the tip.

The over-all compressor performance characteristics were calculated from the weight flow, inlet total pressure, inlet temperature, discharge static pressure, and discharge total temperature, as recommended in reference 4. This method, which is the same as that used in the presentation of the calculated data in the over-all performance investigation of reference 2, does not credit the compressor for nonuniformities of outlet flow velocity and deviation from axial discharge. The individual stage performance was determined from arithmetic averages of total pressure and total temperature at the discharge of each stage in conjunction with the tables of reference 5.

The flow range of any given stage in a multistage compressor cannot be controlled independently of speed because of the choke and surge limit imposed on the compressor at any one speed. In order to correlate the stage data independent of speed, the stage performance is presented in terms of flow coefficient, equivalent pressure ratio, equivalent temperature-rise ratio, and adiabatic efficiency. The equivalent values presented are approximately those that would be obtained if the complete flow range of each stage could have been covered at design speed. Complete derivation of these dimensionless performance parameters is presented in reference 6. The Mach number term in the flow-coefficient parameter was approximated by calculating an approximate Mach number from the outer-wall static pressure and the average total pressure at the entrance to each stage. The exact forms of the parameters as used to calculate the individual stage performance of the compressor can be found in appendix B of reference 7.

Because of compressibility effects, variation in Mach number level, and stage interaction, the equivalent stage curves are not exactly those which would be obtained if the complete range of flow coefficients could be covered at design speed. However, these equivalent curves are useful in determining stage matching and stage performance, inasmuch as each portion of the curves is obtained at the speed at which the stage operates in the multistage compressor.

The absolute magnitudes of the values of the individual stage performance parameters are subject to the usual experimental errors. At low speeds, the temperature and pressure rises across a single stage are small and the speed-correction factor is large, and hence any experimental error is magnified. When a stage is operating far from its design point, the fixed rake instrumentation may be in wakes or unsteady flow regions, with resulting inaccuracies.

The flow coefficient Q/U_mA is the ratio of the volume flow divided by the mean wheel speed and annulus area at the entrance to each stage. In order that the flow coefficient equal the average axial velocity divided by the mean wheel speed, an effective area would have to be used. No data were taken from which the effective area could be determined, and hence it was necessary to use the total annular area. It is believed that the blockage due to wall boundary layer is small and for any given stage remains nearly constant with changes in speed and flow, and hence the flow coefficient as calculated is representative of an average angle of attack on the stage.

The general shape of the stage performance curves and the locations of the peaks and break points probably are unaltered by the inaccuracies in the absolute magnitude of the values obtained.

RESULTS AND DISCUSSION

Compressor Over-All Performance

The over-all performance characteristics of the compressor with interstage instrumentation are presented in figure 3. Total-pressure ratio and adiabatic temperature-rise efficiency are plotted against equivalent weight flow over a range of equivalent speeds from 30 to 100 percent of design. The solid curves are taken from the over-all performance tests of reference 2, and the data points from the interstage tests. The over-all performance data with and without interstage instrumentation agree very well, except for a slight discrepancy in the weight-flow measurements at 80- and 100-percent design speed. This discrepancy is due to the fact that these speeds were run at a different inlet temperature from the tests of reference 2, which resulted in slight errors in the orifice weight-flow measurement.

At design speed a maximum total-pressure ratio of 9.92 was obtained at an equivalent weight flow of 65.7 pounds per second with an efficiency of 0.83. The maximum weight flow obtained at design speed was 66.4 pounds per second. The peak efficiency increased from 0.74 at 30-percent design speed to 0.87 at 80 and 90 percent of design speed and then decreased to 0.83 at design speed.

The surge line in figure 3 is taken from reference 2, since the maximum pressure ratio points of this investigation were slightly below the surge point. There is a knee in the surge line resulting from a sudden change in slope at 63 percent of design speed. A portion of the surge line is dotted, because no data were taken between 60 and 63 percent of design speed. The severity of the surge limitation varies considerably with different compressors, as evidenced by the results of

references 6 and 8. The surge line of this compressor is continuous, and the change in slope at the knee in the surge line is relatively small.

Stage Performance

The volume-flow range of any given stage in a multistage compressor cannot be controlled independently of speed because of the choke and surge limit imposed in the compressor at any one speed. The following stage performance characteristics are presented as equivalent parameters in order to correlate the stage data independently of speed. 3393

Transonic stages 1 and 2. - The performance characteristics of the first stage are presented in figure 4(a). Since no inlet guide vanes were employed and the losses through the inlet bellmouth were negligible, the equivalent performance parameters for this stage were evaluated from the total-pressure and total-temperature conditions of the inlet depression tank and the stage exit. Although the first stage operated over a narrow range of flow coefficient at each equivalent speed, it operated over a very wide range of flow coefficient over the range of speeds investigated. As the speed was decreased, the flow coefficient decreased from a maximum of 0.68 at the design-speed choke-flow point to a minimum of 0.24 at the 30-percent-speed surge point. This wide range of flow coefficient results in first-stage operation over a very wide range of angle of attack. The inlet stage operated at least partially stalled below a flow coefficient of approximately 0.45, as indicated by the rapid rise in equivalent temperature-rise ratio and the rapid decrease in equivalent total-pressure ratio at flow coefficients below this value. The approximate surge points, denoted by the solid symbols, indicate that the inlet stage became stalled along the surge line between 60 and 70 percent of equivalent design speed; this result correlates with the abrupt change in the slope of the compressor surge line shown in figure 3. To illustrate the area of compressor operation in which inlet-stage stall was encountered, the approximate first-stage stall line is included in figure 3.

From the data in figure 4(a), it is apparent that at 60 percent of equivalent design speed the inlet stage operated unstalled when the compressor was choked; but, as the weight flow was decreased at that speed, the angle of attack increased until some portion of the blade span stalled, probably resulting in rotating stall. At all operating conditions to the left of the first-stage stall line shown in figure 3, the first stage was operating stalled. As a result of the rapid decrease in pressure rise and the rapid increase in energy addition across the first stage at values of flow coefficient below 0.45, there was a sharp decrease in the efficiency of the first stage at equivalent speeds below 60 percent of design.

At design speed, the equivalent pressure ratio of the first stage was slightly less than the design value; and at 90 percent of equivalent design speed, the equivalent pressure ratio was slightly higher than the

design value. Consequently, the design equivalent pressure ratio was attained only over a narrow speed range between 90 and 100 percent of equivalent design speed. For comparison, the design pressure ratio is shown on figure 4; however, since the boundary-layer blockage cannot be evaluated accurately, no comparison between measured and design flow coefficient can be made.

The second-stage performance characteristics are presented in figure 4(b). The range of flow coefficient at a constant equivalent speed and over the range of equivalent speed investigated is of the same magnitude and follows the same general trend as in the first stage. Although the second stage appears to stall over approximately the same range of equivalent speeds and compressor-inlet flow conditions as does the first, stall is not as clearly defined by the rapid decrease in equivalent total-pressure ratio and increase in equivalent temperature-rise ratio as in the first stage. At all second-stage flow coefficients below approximately 0.45, the first stage is operating stalled, and the second-stage stall may be an interaction effect. In addition, the large margin between design and peak equivalent total-pressure ratio, which was characteristic of the first stage, does not occur in the second stage. The second-stage peak equivalent total-pressure ratio of approximately 1.385 was only slightly higher than the design total-pressure ratio; this narrow margin between peak and design total-pressure ratios would not be expected in a stage composed of blades with sections designed to operate at their minimum-loss points.

3393

The design diffusion factors for this stage (ref. 1) are less than the recommended blade tip limit of 0.45 for efficiencies above 0.90 given in reference 9, and hence the poor performance of this stage cannot be attributed to high stage design loading. Both the low peak equivalent total-pressure ratio and the small decrease below the peak equivalent total-pressure ratio in the low-flow-coefficient range could be caused by a mismatching of the various blade elements due to a maldistribution of axial velocity set up by the large change in hub curvature preceding this stage (ref. 10). It has been shown (ref. 11) that the effect of closing the first-stage stators would be to shift the second-stage curve downward and to the left; that is, toward lower pressure ratios and flow coefficients. Hence, the low equivalent pressure ratio of this stage may be due to an improper first-stage stator blade setting.

Intermediate stages 3 to 6. - The individual stage performance curves for stages 3 to 6 are presented in figures 4(c) to (f). The range of flow coefficient over which each of these stages operates decreases from the third to the sixth stage. The range of flow coefficient covered at any constant equivalent speed generally increases from the third to the sixth stage, with the range at low speeds extending to lower flow coefficients, until in the sixth stage most of the stage flow-coefficient range is covered at each of the equivalent speeds investigated. In the third, fourth, and fifth stages, there is a decrease in pressure ratio from the

peak at the low flow coefficients at 30, 50, and 60 percent of design speed. These operating points are to the left of the first-stage stall line in figure 3, and this decrease in pressure ratio may be due to first-stage stall interaction effects or to high-angle-of-attack stall of these stages. These first-stage stall interaction effects did not cause a sudden drop in the performance of these stages at low flow coefficients as discussed in references 3 and 6. The sixth stage, in operating over a very small range of flow coefficient, remains unstalled for all speeds and flow conditions covered in this investigation. These stage curves show a peak equivalent total-pressure ratio appreciably higher than the design pressure ratio, as would be expected from the cascade data for blades designed for an angle of attack for minimum loss (ref. 1), indicating that the various radial blade elements are probably well matched and that the flow distribution entering these stages approaches design flow conditions at the design flow coefficient.

The design equivalent pressure ratio was attained over an increasingly wide range of speeds from the third to the sixth stage; in the sixth stage the design equivalent pressure ratio was attained over the entire range of speeds investigated. The equivalent-temperature-rise-ratio curves show that, with the exception of the fourth stage, the design equivalent temperature-rise ratio was obtained at the design pressure ratio. Since the fourth stage produced greater than design temperature-rise ratio at the design pressure ratio, the actual efficiency is lower than the design value at this flow coefficient for this stage. However, the indicated efficiencies of the third stage are unusually high, and it is believed that the temperature measurements at the exit of the third stage were somewhat low. As a result, the calculated efficiencies of the third stage were too high, and of the fourth stage, too low.

The design tip diffusion factor of 0.51 for the sixth stage is appreciably above the recommended limit of 0.45 for efficiencies above 0.90 (ref. 9). However, the efficiency of this stage at the design pressure ratio remained high, indicating that tip diffusion factors above the recommended limit can be used in the latter stages of a multistage compressor. However, high tip design diffusion factor, while not appreciably lowering the over-all stage efficiency, may set up radial entropy gradients that produce axial-velocity gradients (ref. 10) that could adversely affect later stages.

Exit stages 7 and 8. - The performance characteristics of the seventh stage are presented in figure 4(g). The range of flow coefficient over which the seventh stage operates is greater than that covered in any of the intermediate stages (fig. 5). However, this stage operates almost exclusively on the negative-slope side of its equivalent total-pressure-ratio curve. It operates on the positive-slope (positive-stall) side of its equivalent total-pressure ratio curve at the 90- and 100-percent-speed surge points. As the speed is decreased from design, the flow coefficient increases from a minimum of 0.45 at the design-speed surge point to a maximum of 0.80 at the 30-percent-speed choked-flow point.

Both the total-pressure and the temperature-rise ratios of the seventh stage peak at approximately the design values, which would not be expected from blades designed to operate at the minimum-loss point. This deficiency in energy addition and pressure rise is probably due to a poor radial distribution of the flow entering this stage, which results in a mismatching of the various blade elements (ref. 11).

At the design pressure ratio at design speed, the efficiency of the seventh stage was good, even though the design tip diffusion factor of 0.52 for this stage is higher (ref. 1) than the limiting value of 0.45 for efficiencies above 0.90 (ref. 9).

3393

The eighth-stage performance characteristics are presented in figure 4(h). The required range of flow coefficient covered by this stage is somewhat greater than that required of the seventh stage; however, the range of flow coefficient at any constant equivalent speed is of the same general magnitude and follows the same general trend as in the seventh stage, with the maximum flow coefficient occurring at the 30-percent-speed choke point. The choked-flow coefficient for the eighth stage at 50-percent speed is approximately 0.82, whereas at design speed it is only 0.63. The low-angle-of-attack stall of 65-series blades will occur at higher angles of attack at higher Mach numbers, and hence the stage will choke at decreasing flow coefficients with increasing speed. In this stage, as in the seventh, the 90- and 100-percent-speed surge points are on the positive-slope (positive-stall) side of the equivalent total-pressure-ratio curve. At the flow coefficient at which the eighth stage produced the design equivalent temperature-rise ratio, the equivalent pressure ratio was somewhat below the design value. The peak equivalent total-pressure ratio was approximately equal to the design pressure ratio, as in the seventh stage; while the equivalent temperature-rise ratio extended appreciably above the design value.

2-10

The design tip diffusion factor of 0.54 for this stage (ref. 1) is appreciably higher than the recommended limit of 0.45 for efficiencies above 0.90 (ref. 9). It is believed that this did not cause the low efficiencies in the stage, because the efficiencies at part speeds, where the actual diffusion factors would be low, are not appreciably different from those at design speed. The poor performance of the eighth stage is probably due to axial-velocity distribution appreciably different from design because of boundary-layer build-up and radial entropy gradients developed by preceding stages (refs. 10 and 11), which could result from the high design diffusion factor of preceding stages.

Stage Matching

The individual stage curves of equivalent total-pressure ratio against flow coefficient are presented in figure 6. These curves were faired from

the data points of figure 4, and for clarity only a few selected operating points are shown. The operating point (solid symbol) for design-speed maximum total-pressure ratio most nearly approaches the over-all compressor design point. No allowance was made for boundary-layer blockage at the entrance to the first stage in the design; and, because the design weight flow was obtained and some boundary layer must exist at this station, lower than design loading of the first stage is indicated. At this operating point the first-stage pressure ratio is below design, which would result in a flow coefficient entering the second stage that is higher than design, if the design passage area were correct. The temperature ratio across a stage, of course, also affects the flow coefficient entering the next stage, but to a smaller degree than the pressure ratio. To account for both pressure and temperature effects, the density ratio entering each stage for this point is compared with the design value in figure 7. These are total-density ratios, but, because the velocities are of the same order of magnitude throughout the compressor, they should be comparable to the static-density ratios. The higher than design flow coefficient entering the second stage makes this stage operate towards the choke-flow end of its stage curve at a lower than design pressure ratio. The lower than design pressure ratio of the first two stages could be expected to make the third stage operate at a much higher than design flow coefficient and resulting lower than design pressure ratio. If the design boundary-layer blockage allowance were correct throughout the compressor, the density ratios in figure 7 would diverge from design stagewise through the compressor. However, this did not occur, and the third and fourth stages are producing design pressure ratio and the fifth and sixth stages higher than design pressure ratio. Hence, the design boundary-layer allowance was too large in these stages, which made them operate near or below their design flow coefficient.

3393

Even though the density ratio entering the seventh and eighth stages was approximately on design, these stages operated at the high-angle-of-attack stall end of their curves, because the passage area was too large and resulted in a flow coefficient below design. As a result of this excessive boundary-layer allowance, the stages are mismatched at the point of design-speed maximum pressure ratio, with the two inlet stages operating down on the choked-flow end of their curve and the latter two stages operating over the peak-pressure-ratio point at stall. The over-all compressor design pressure ratio was not obtained, because the seventh and eighth stages stalled before the inlet stages could reach their design operating point.

At the points of 80 and 90 percent of design speed shown in figure 6, the stages are much better matched. At these speeds the first and second stages and the seventh and eighth stages are not operating at the extremities of their stage curves. All the stages are operating on the negative-slope side of their stage curves at a favorable angle of attack. Thus, the stages are more properly matched at some speed below design speed. That the stages are well matched at the 80- and 90-percent speeds

results in a high over-all compressor efficiency for these speeds, as shown in figure 3. In addition, this mismatching, which caused the inlet stages to operate at the design-speed maximum pressure ratio on the choked-flow end of their stage curves and the outlet stages to operate on the positive-slope side of their performance curves, favorably affected the low-speed efficiency.

The design stage efficiency and boundary-layer blockage allowance assumptions can seriously affect the stage matching. The assumed design stage efficiencies were close to the actual performance efficiencies, but it is apparent that the design boundary-layer blockage allowance was much too large. This adversely affected the design-speed performance but helped the low-speed performance.

3393

CI-2 back

CONCLUDING REMARKS

The following results were obtained from an investigation of the individual stage performance of an eight-stage compressor having two transonic inlet stages.

Stages 1, 3, 4, 5, and 6 operated as anticipated in their design, produced a peak equivalent pressure ratio appreciably above the design pressure ratio, and had high efficiencies. Stages 2, 7, and 8 produced a peak equivalent pressure ratio approximately equal to design; and, since the peak pressure ratio would be expected to occur at higher than design angle of attack, the pressure ratio was below design at design angle of attack.

At design-speed maximum pressure ratio, the stages were mismatched because of an excessive design boundary-layer allowance that caused the seventh and eighth stages to stall before design pressure ratio could be obtained. This mismatching at design speed caused a decrease in peak efficiency from 90-percent speed to design speed. The stages were well matched at 80- and 90-percent speed, which resulted in high peak efficiencies at these speeds.

The knee in the surge line at approximately 63 percent of design speed corresponds to the point at which the first stage became unstalled. The excessive design boundary-layer allowance in the rear stages lowered the speed at which the first stage became unstalled and favorably affected the low-speed efficiency. The equivalent pressure ratio of the third, fourth, and fifth stages decreased at low flow coefficients, probably because of high-angle-of-attack stall and first-stage stall interaction effects.

Although the design tip diffusion factors of stages 5 to 8 were higher than those recommended in reference 9, the efficiencies remained high. However, the high design diffusion factors of the intermediate stages could

have set up radial entropy gradients that would produce axial-velocity gradients in the latter stages and adversely affect their performance.

Lewis Flight Propulsion Laboratory
National Advisory Committee for Aeronautics
Cleveland, Ohio, August 17, 1954

3393

REFERENCES

1. Voit, Charles H.: Investigation of a High-Pressure-Ratio Eight-Stage Axial-Flow Research Compressor with Two Transonic Inlet Stages. I - Aerodynamic Design. NACA RM E53I24, 1953.

2. Geye, Richard P., Budinger, Ray E., and Voit, Charles H.: Investigation of a High-Pressure-Ratio Eight-Stage Axial-Flow Research Compressor with Two Transonic Inlet Stages. II - Preliminary Analysis of Over-All Performance. NACA RM E53J06, 1953.

3. Benser, William A.: Analysis of Part-Speed Operation for High-Pressure-Ratio Multistage Axial-Flow Compressors. NACA RM E53I15, 1953.

4. NACA Subcommittee on Compressors: Standard Procedures for Rating and Testing Multistage Axial-Flow Compressors. NACA TN 1138, 1946.

5. Keenan, Joseph H., and Kaye, Joseph: Thermodynamic Properties of Air. John Wiley & Sons, Inc., 1947.

6. Medeiros, Arthur A., Benser, William A., and Hatch, James E.: Analysis of Off-Design Performance of a 16-Stage Axial-Flow Compressor with Various Blade Modifications. NACA RM E52L03, 1953.

7. Budinger, Ray E., and Serovy, George K.: Investigation of a 10-Stage Subsonic Axial-Flow Research Compressor. IV - Individual Stage Performance Characteristics. NACA RM E53C11, 1953.

8. Lucas, James G., Finger, Harold B., and Filippi, Richard E.: Effect of Inlet-Annulus Area Blockage on Over-All Performance and Stall Characteristics of an Experimental 15-Stage Axial-Flow Compressor. NACA RM E53L28, 1954.

9. Lieblein, Seymour, Schwenk, Francis C., and Broderick, Robert L.: Diffusion Factor for Estimating Losses and Limiting Blade Loadings in Axial-Flow-Compressor Blade Elements. NACA RM E53D01, 1953.

10. Hatch, James E., Giamati, Charles C., and Jackson, Robert J.: Application of Radial-Equilibrium Condition to Axial-Flow Turbomachine Design Including Consideration of Change of Entropy with Radius Downstream of Blade Row. NACA RM E54A20, 1954.

11. Budinger, Ray E.: Investigation of a 10-Stage Subsonic Axial-Flow Research Compressor. VI - Performance Evaluation and Flow Distributions in the First, Fifth, and Tenth Stages. NACA RM E54F28, 1954.

3393

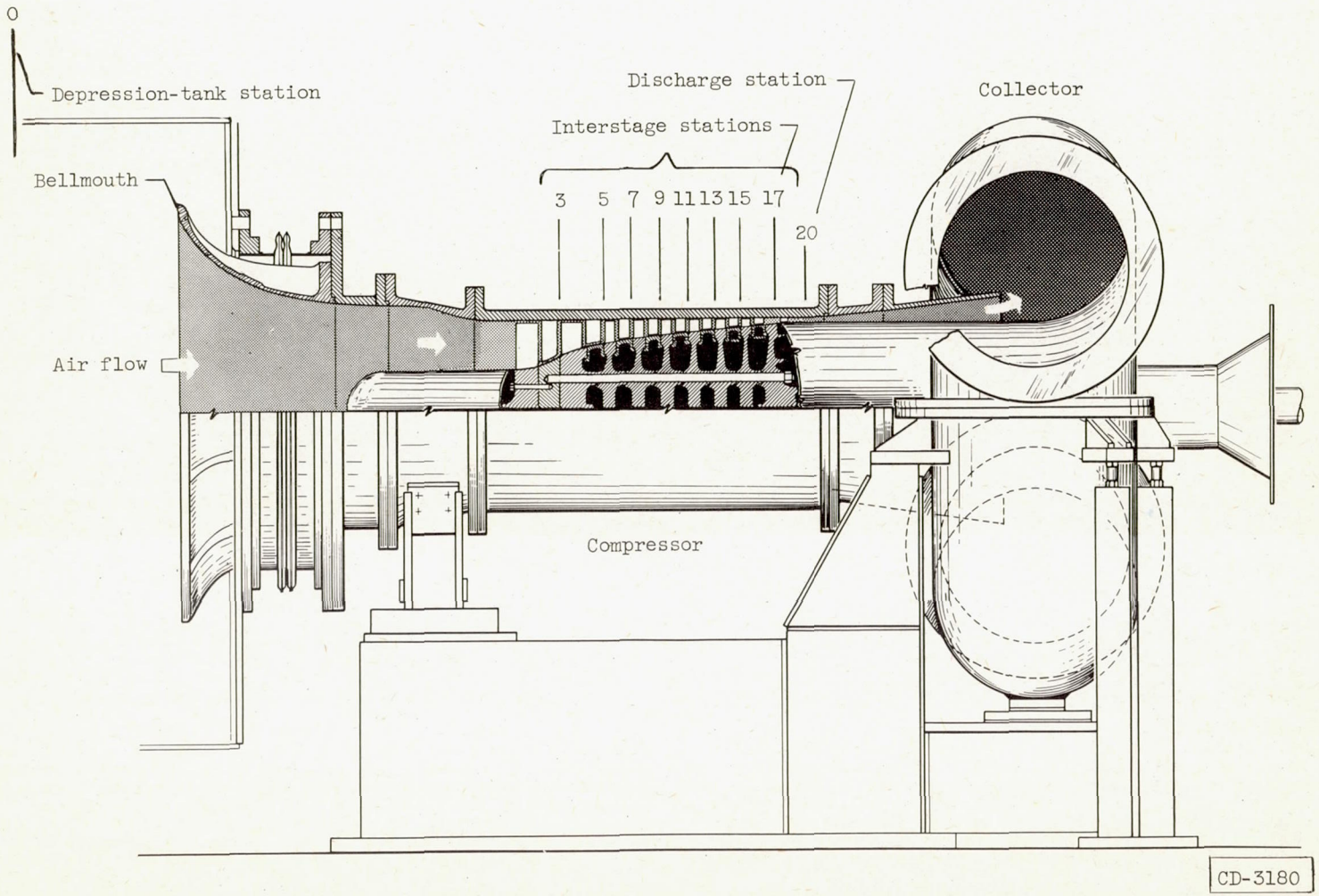

Figure 1. - Cross-sectional view of eight-stage axial-flow compressor, inlet bellmouth, and discharge collector.

3393

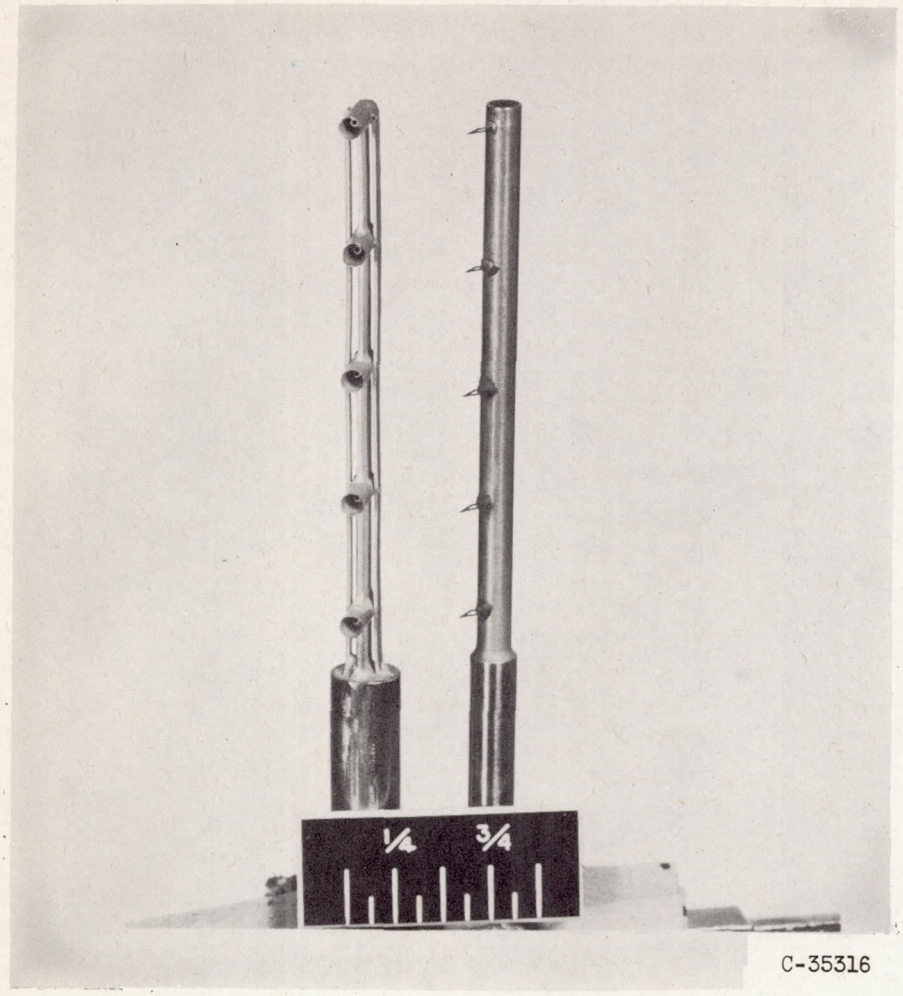

(a) Total-pressure rake.

(b) Total-temperature rake.

Figure 2. - Typical radial rake instrumentation used to determine stage performance characteristics.

3393

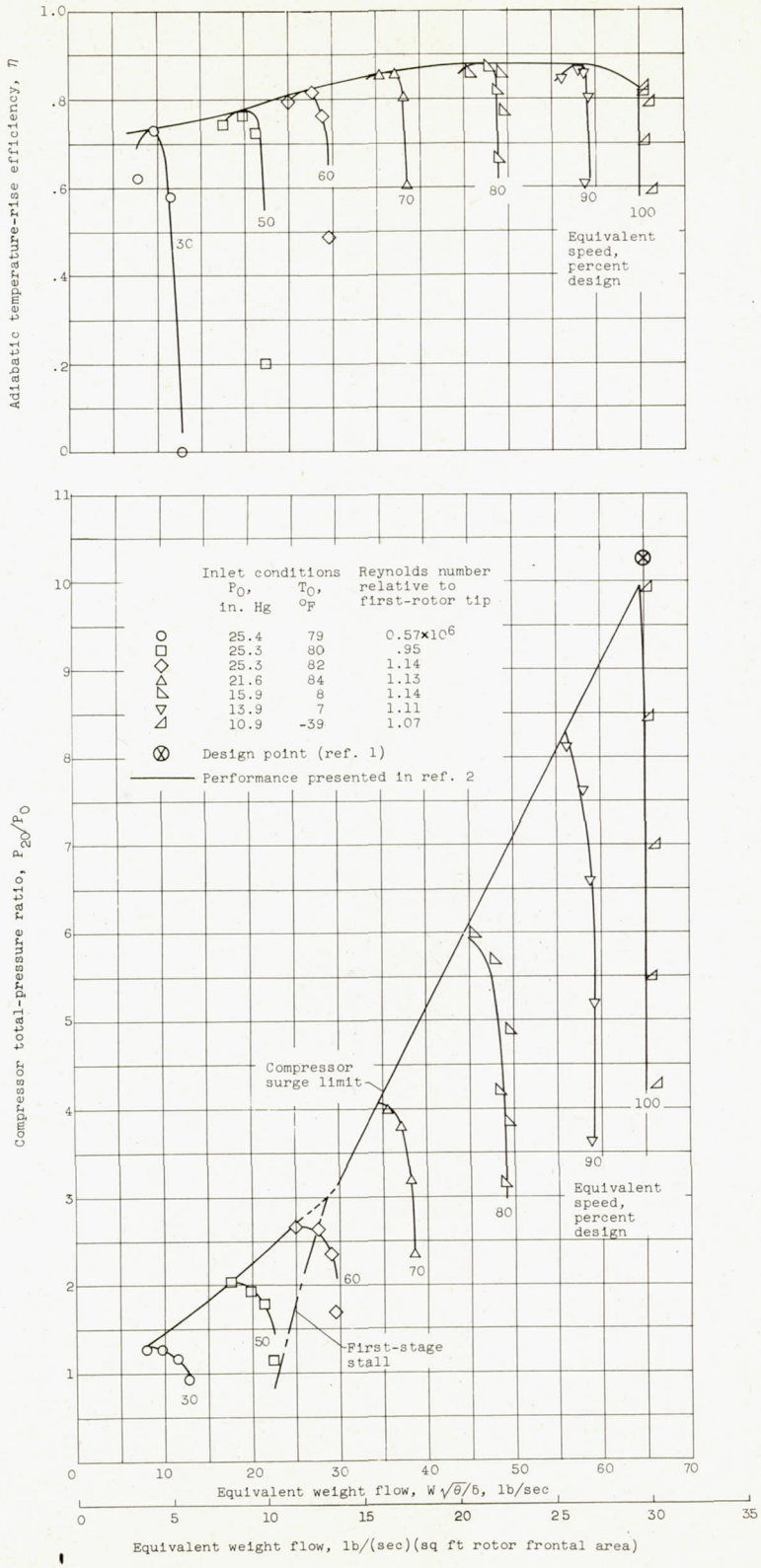

Figure 3. - Over-all performance characteristics of eight-stage axial-flow compressor.

CI-3 3393

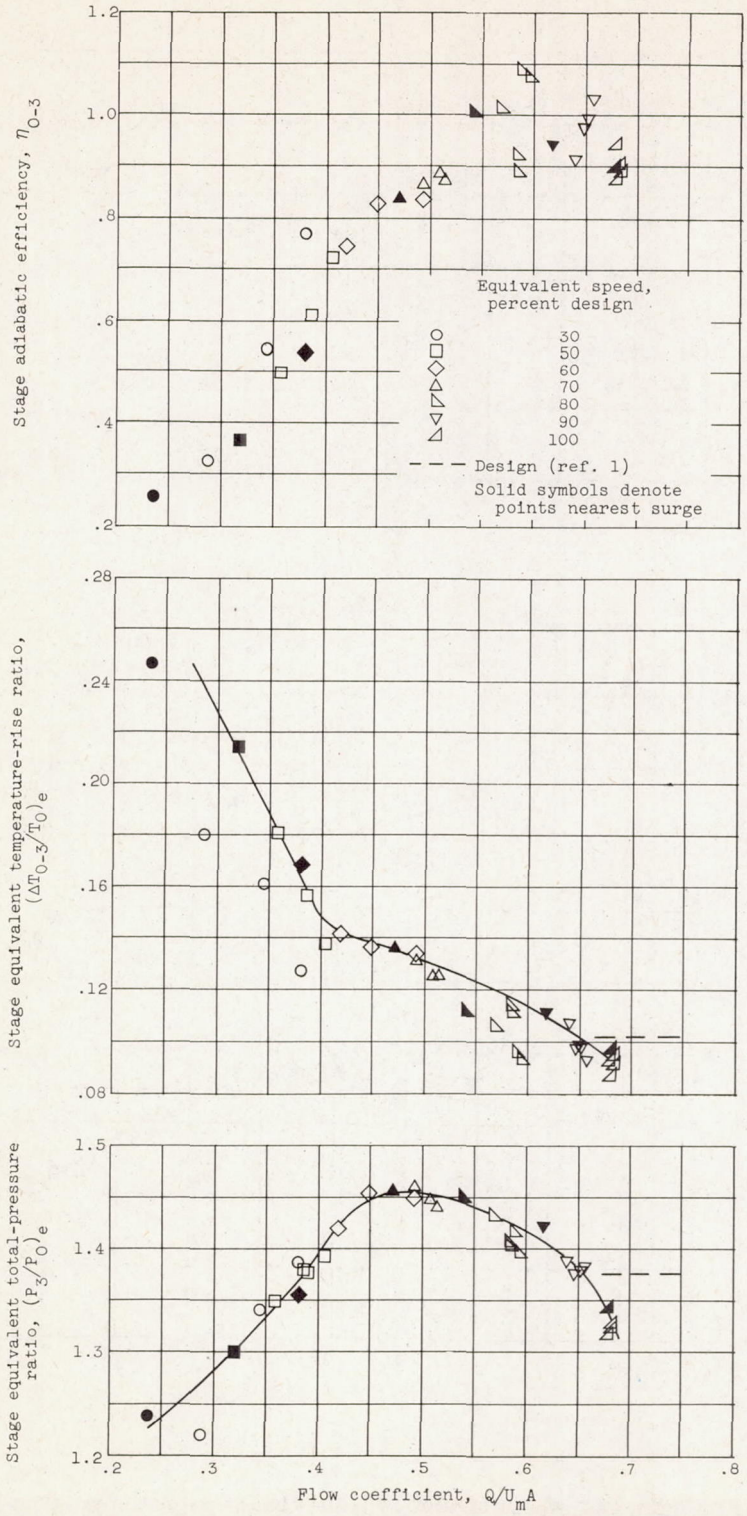

(a) First stage.

Figure 4. - Individual stage performance of eight-stage compressor over entire flow range at speeds from 30 to 100 percent of equivalent design speed.

3393

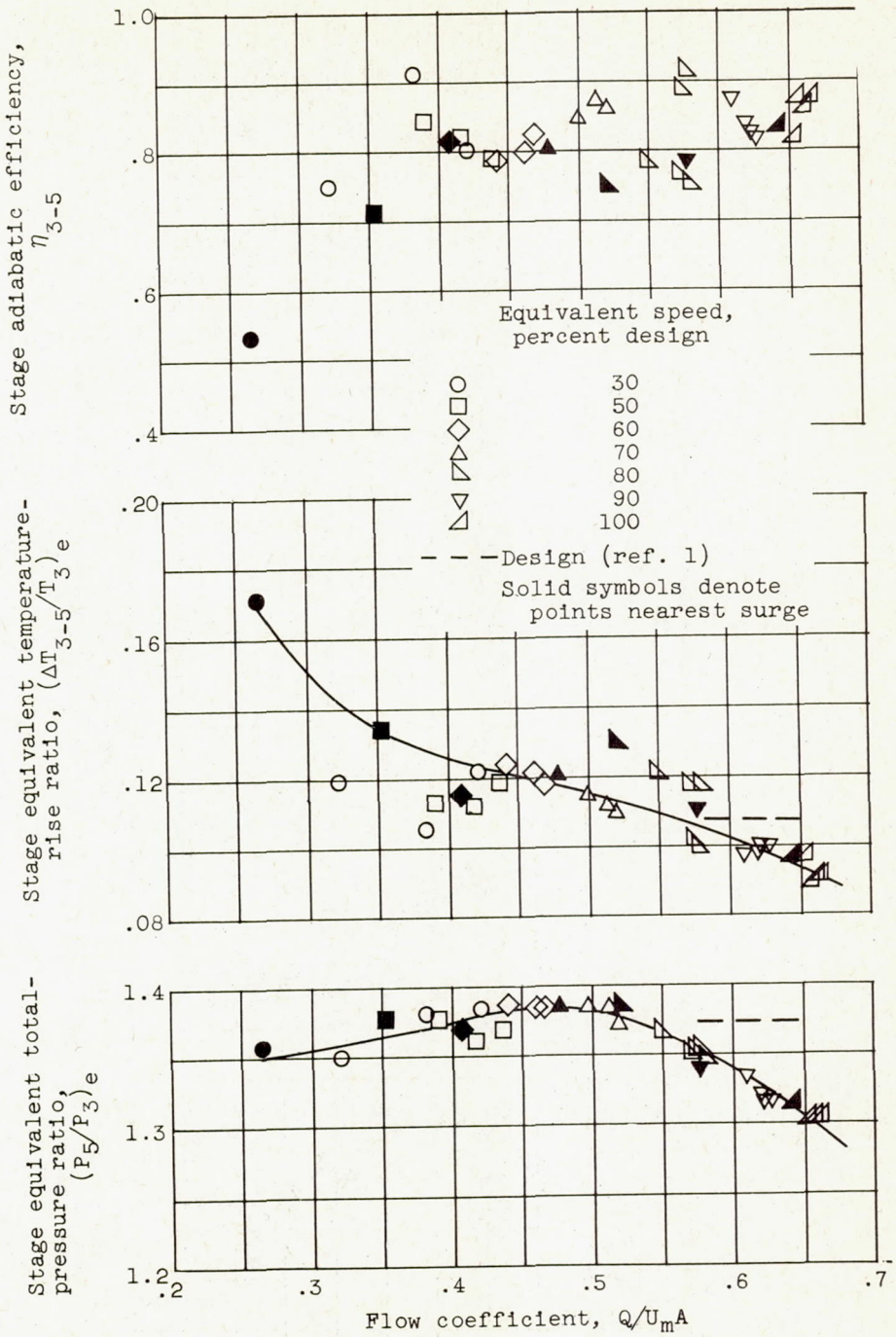

(b) Second stage.

Figure 4. - Continued. Individual stage performance of eight-stage compressor over entire flow range at speeds from 30 to 100 percent of equivalent design speed.

C1-3 back 3393

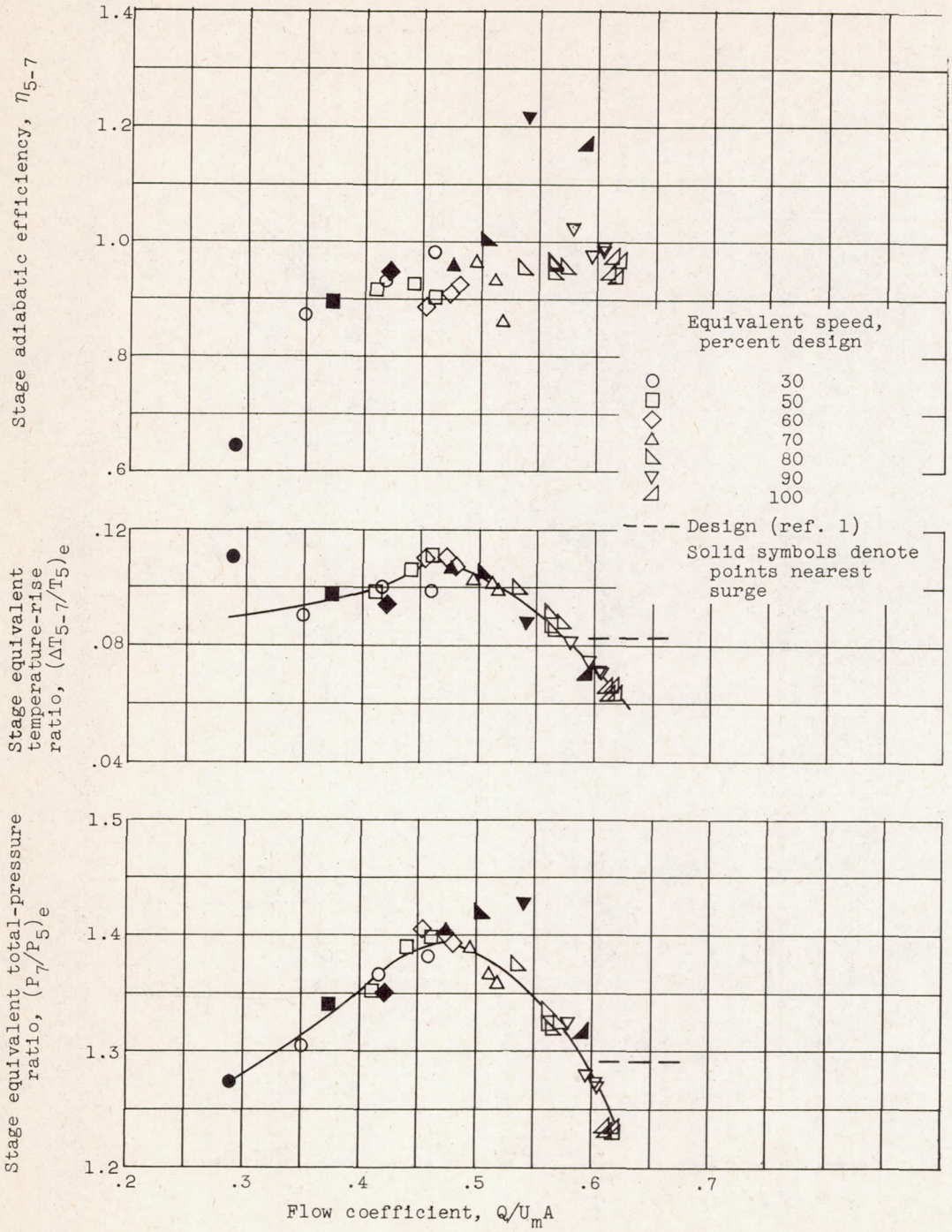

(c) Third stage.

Figure 4. - Continued. Individual stage performance of eight-stage compressor over entire flow range at speeds from 30 to 100 percent of equivalent design speed.

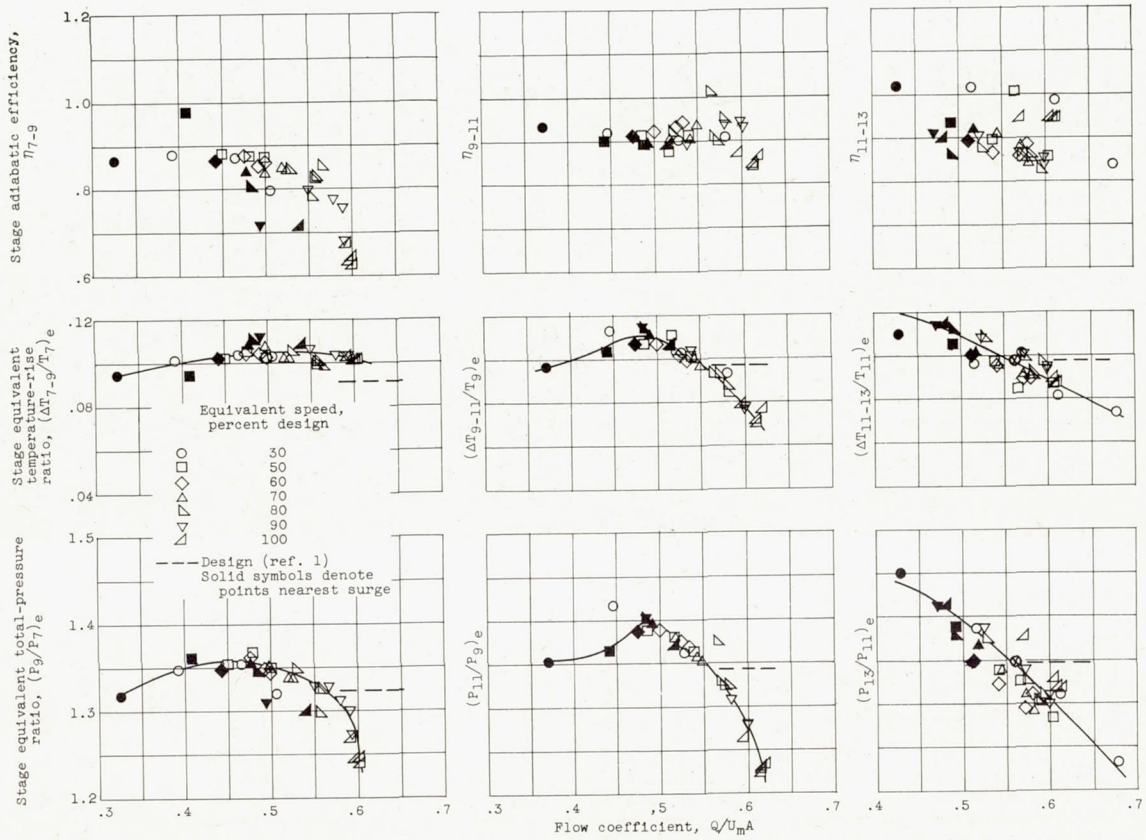

(d) Fourth stage. (e) Fifth stage. (f) Sixth stage.

Figure 4. - Continued. Individual stage performance of eight-stage compressor over entire flow range at speeds from 30 to 100 percent of equivalent design speed.

3393

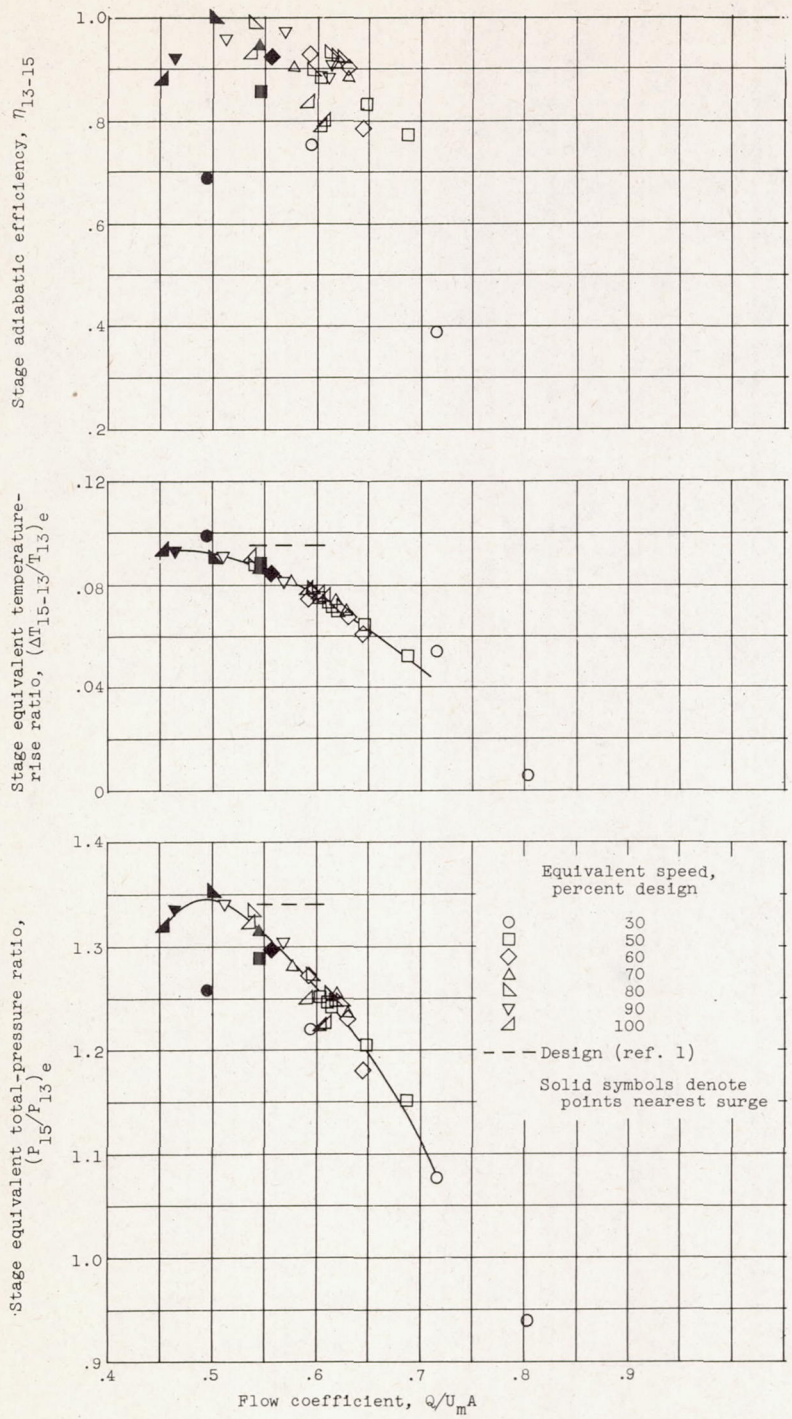

(g) Seventh stage.

Figure 4. - Continued. Individual stage performance of eight-stage compressor over entire flow range at speeds from 30 to 100 percent of equivalent design speed.

3393

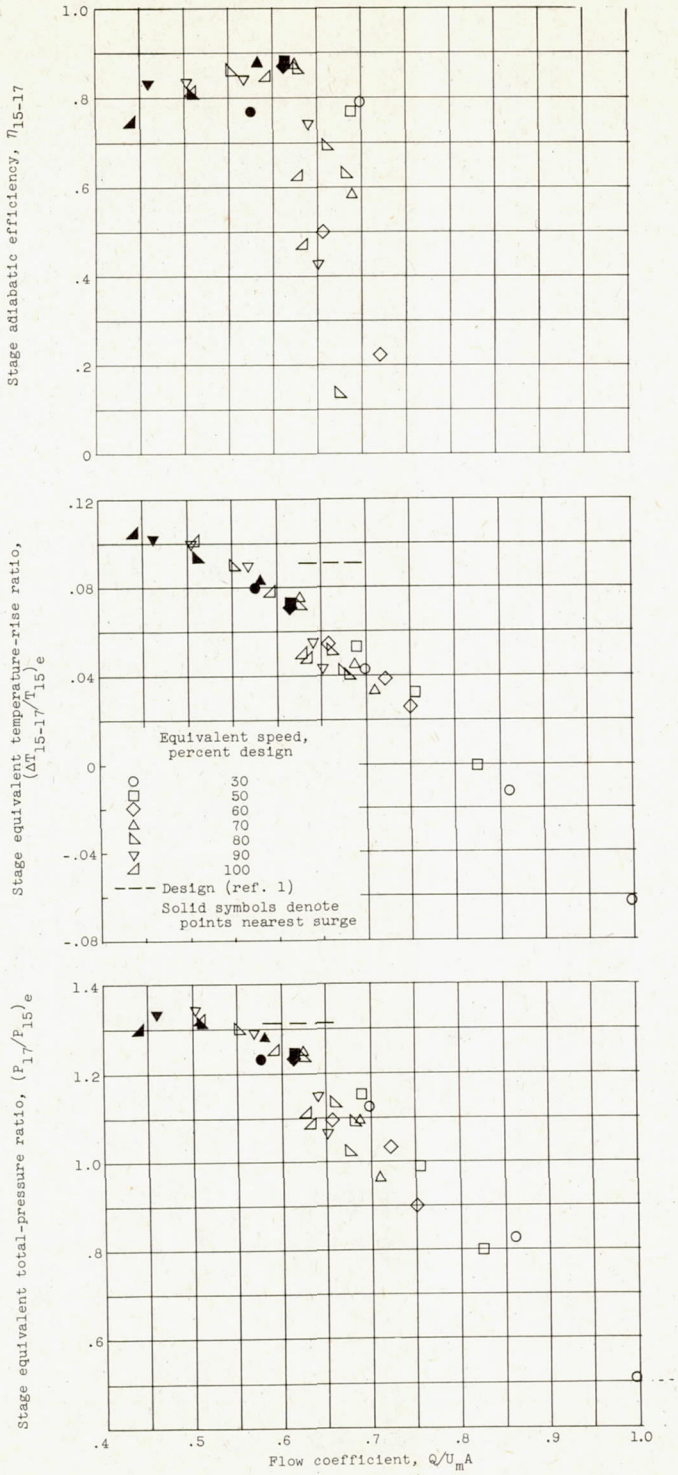

(h) Eighth stage.

Figure 4. - Concluded. Individual stage performance of eight-stage compressor over entire flow range at speeds from 30 to 100 percent of equivalent design speed.

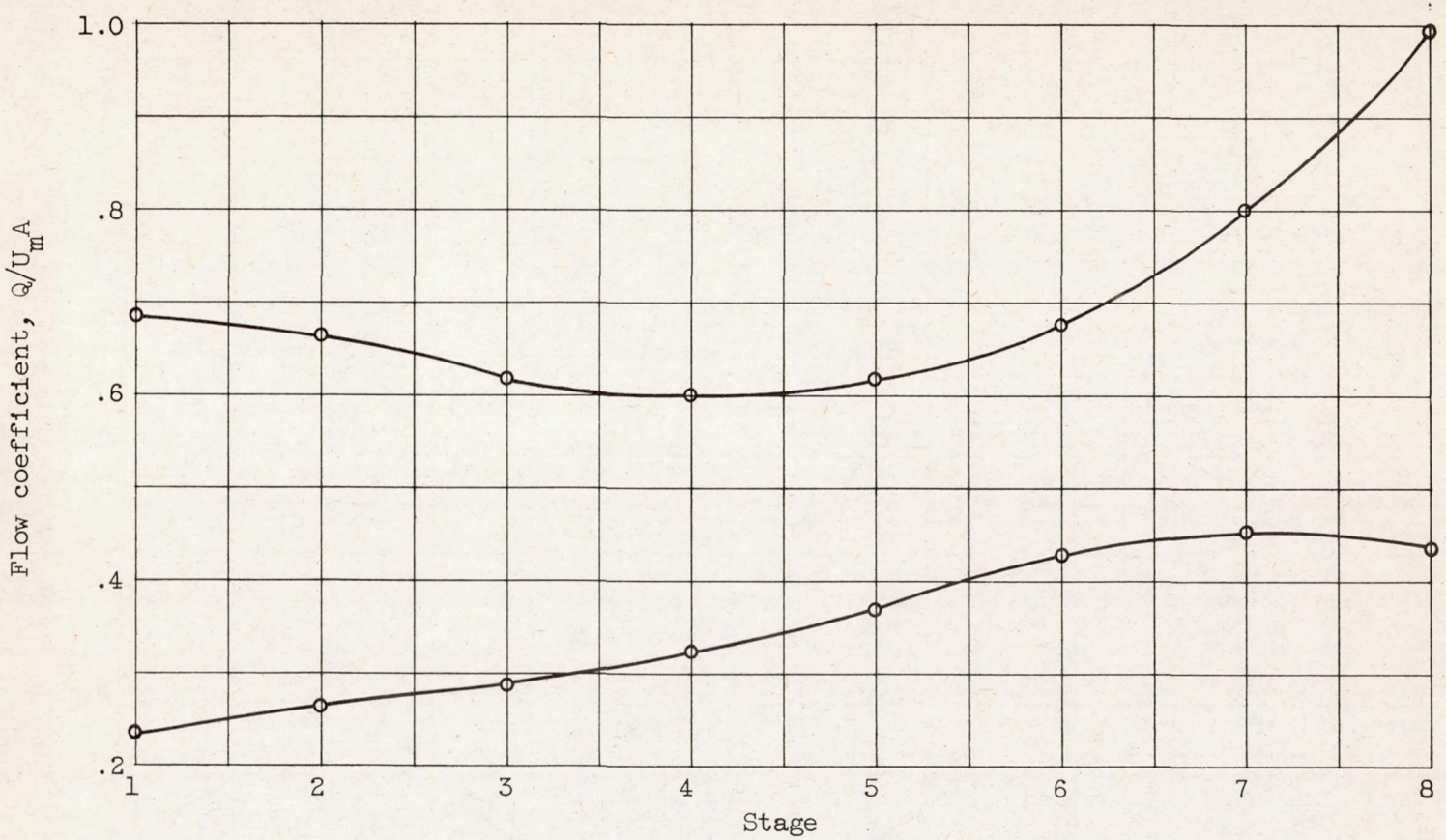

Figure 5. - Maximum flow-coefficient range of individual stages from 30- to 100-percent design speed.

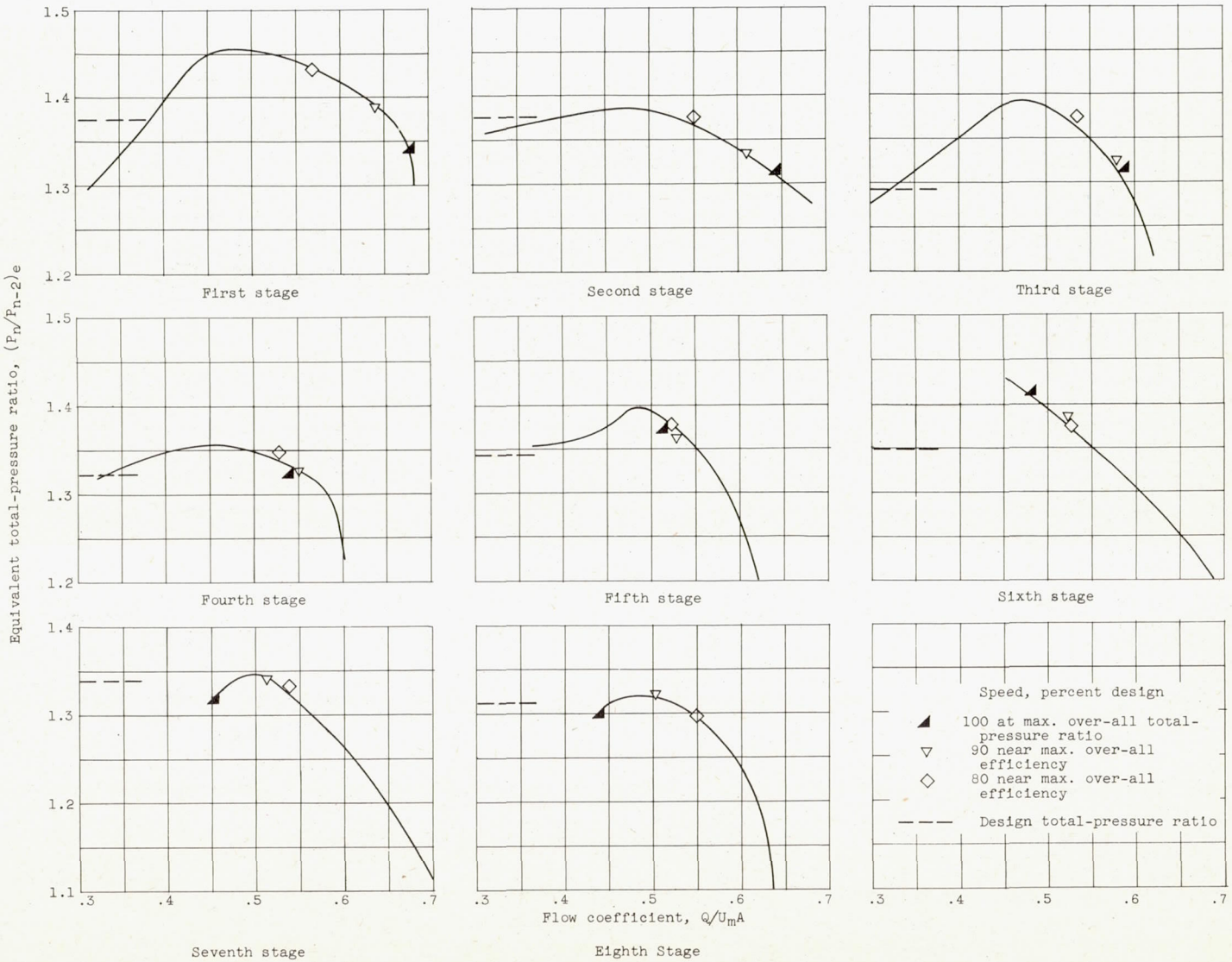

Figure 6. - Individual stage performance curves faired from data points of figure 4.

3393

CI-4

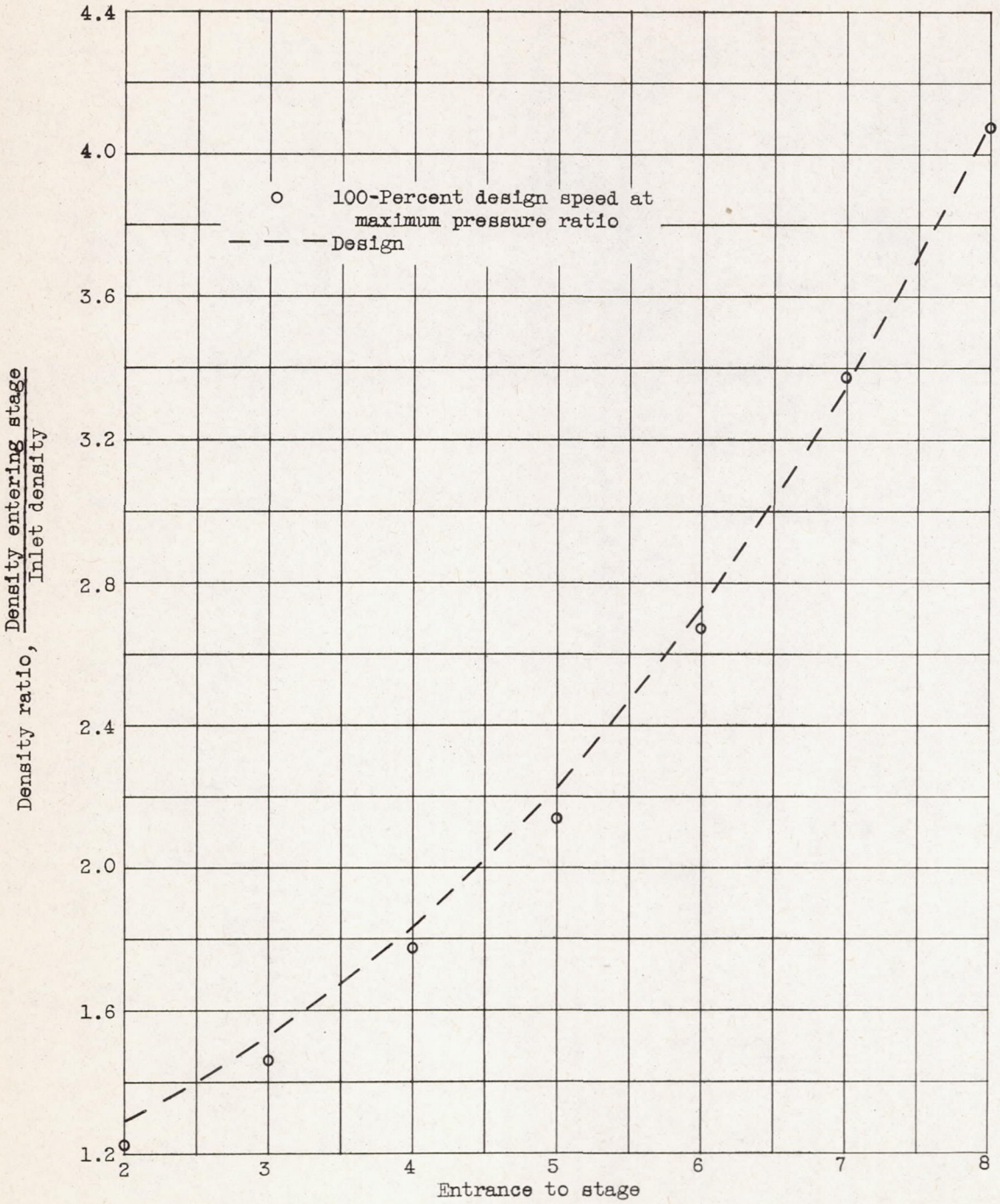

Figure 7. - Comparison of density ratio entering each stage with design value.